

## Co-expression network analysis identified hub genes critical to triglyceride and free fatty acid metabolism as key regulators of age-related vascular dysfunction in mice

Huimin Li<sup>1,2,\*</sup>, Xinhui Wang<sup>3,\*</sup>, Xinyue Lu<sup>1</sup>, Hongxin Zhu<sup>1</sup>, Sheng Li<sup>1</sup>, Shiwei Duan<sup>4</sup>, Xinzhi Zhao<sup>5</sup>, Fuquan Zhang<sup>6</sup>, Gil Alterovitz<sup>2</sup>, Fudi Wang<sup>3</sup>, Qiang Li<sup>7</sup>, Xiao-Li Tian<sup>8</sup>, Mingqing Xu<sup>1,2</sup>

<sup>1</sup>Bio-X Institutes, Key Laboratory for the Genetics of Developmental and Neuropsychiatric Disorders (Ministry of Education), Shanghai Jiao Tong University, Shanghai 200030, China

<sup>2</sup>Center for Biomedical Informatics, Harvard Medical School, Boston, MA 02115, USA

<sup>3</sup>School of Public Health, The First Affiliated Hospital, Institute of Translational Medicine, Zhejiang University School of Medicine, Hangzhou 310058, China

<sup>4</sup>Medical Genetics Center, School of Medicine, Ningbo University, Ningbo 315000, Zhejiang, China

<sup>5</sup>International Peace Maternity and Child Health Hospital of China Affiliated to Shanghai Jiao Tong University, Shanghai 200030, China

<sup>6</sup>Wuxi Mental Health Center, Wuxi 214000, China

<sup>7</sup>Translational Medical Center for Development and Disease, Institute of Pediatrics, Shanghai Key Laboratory of Birth Defect, Children's Hospital of Fudan University, Shanghai 201102, China

<sup>8</sup>Department of Human Population Genetics, Human Aging Research Institute and School of Life Science, Nanchang University, Nanchang 330031, China

\*Equal contribution

**Correspondence to:** Mingqing Xu, Xiao-Li Tian; email: [mingqingxu@gmail.com](mailto:mingqingxu@gmail.com), [tianxiaoli@ncu.edu.cn](mailto:tianxiaoli@ncu.edu.cn)

**Keywords:** co-expression network, hub gene, module, aging, vascular dysfunction, mouse

**Received:** July 8, 2019

**Accepted:** September 5, 2019

**Published:** September 12, 2019

**Copyright:** Li et al. This is an open-access article distributed under the terms of the Creative Commons Attribution License (CC BY 3.0), which permits unrestricted use, distribution, and reproduction in any medium, provided the original author and source are credited.

### ABSTRACT

**Background:** Aging has often been linked to age-related vascular disorders. The elucidation of the putative genes and pathways underlying vascular aging likely provides useful insights into vascular diseases at advanced ages. Transcriptional regulatory network analysis is the key to describing genetic interactions between molecular regulators and their target gene transcriptionally changed during vascular aging.

**Results:** A total of 469 differentially expressed genes were parsed into 6 modules. Among the incorporated sample traits, the most significant module related to vascular aging was associated with triglyceride and enriched with biological terms like proteolysis, blood circulation, and circulatory system process. The module associated with triglyceride was preserved in an independent microarray dataset, indicating the robustness of the identified vascular aging-related subnetwork. Additionally, *Enpp5*, *Fez1*, *Kif1a*, *F3*, *H2-Q7*, and their interacting miRNAs *mmu-miR-449a*, *mmu-miR-449c*, *mmu-miR-34c*, *mmu-miR-34b-5p*, *mmu-miR-15a*, and *mmu-let-7*, exhibited the most connectivity with external lipid-related traits. Transcriptional alterations of the hub genes *Enpp5*, *Fez1*, *Kif1a*, and *F3*, and the interacting microRNAs *mmu-miR-34c*, *mmu-miR-34b-5p*, *mmu-let-7*, *mmu-miR-449a*, and *mmu-miR-449c* were confirmed.

**Conclusion:** Our findings demonstrate that triglyceride and free fatty acid-related genes are key regulators of age-related vascular dysfunction in mice and show that the hub genes for *Enpp5*, *Fez1*, *Kif1a*, and *F3* as well as

their interacting miRNAs mmu-miR-34c, mmu-miR-34b-5p, mmu-let-7, mmu-miR-449a, and mmu-miR-449c, could serve as potential biomarkers in vascular aging.

**Methods:** The microarray gene expression profiles of aorta samples from 6-month old mice (n=6) and 20-month old mice (n=6) were processed to identify nominal differentially expressed genes. These nominal differentially expressed genes were subjected to a weighted gene co-expression network analysis. A network-driven integrative analysis with microRNAs and transcription factors was performed to define significant modules and underlying regulatory pathways associated with vascular aging, and module preservation test was conducted to validate the age-related modules based on an independent microarray gene expression dataset in mice aorta samples including three 32-week old wild-type mice (around 6-month old) and three 78-week old wild-type mice (around 20-month old). Gene ontology and protein-protein interaction analyses were conducted to determine the hub genes as potential biomarkers in the progress of vascular aging. The hub genes were further validated with quantitative real-time polymerase chain reaction in aorta samples from 20 young (6-month old) mice and 20 old (20-month old) mice.

## INTRODUCTION

Vascular aging is characterized by structural and functional alterations of the vascular wall, deteriorating vascular integrity and vessel homeostasis, including increased luminal diameter with wall remodeling and augmented intimal and medial thickening, reorganization of the extracellular matrix with altered collagen, and elastin content and calcifications [1]. These changes may increase cardiovascular morbidity and mortality by leading unequivocally to a number of detrimental changes in the cardiovascular system that are discriminated with atherosclerotic pathology [2]. These age-related vascular diseases remain a leading cause of mortality and account for 40% of overall deaths worldwide [3]. Aging-induced aorta stiffening was demonstrated to be a natural consequence of increasing age that might be due to the several impairments including alteration in aortic wall [4]. The development of physiological vascular aging is subjected to the alterations in the function of the endothelium that line the lumen of blood vessels, which are mediated through both genetic and environmental factors [5–7]. At the cellular level, decreased protein synthesis, increased angiotensin II levels, mitochondrial dysfunction, autophagy, altered pattern of calcium regulation and increased DNA, protein, and lipid oxidation are mainly observed [8–10]. Additionally, it is evident that processes involving immune responses and oxidative stress occur in vascular aging [11].

The elucidation of the putative genes and pathways underlying vascular aging is critical for understanding the molecular mechanisms of age-related vascular diseases. Previous research has discussed the roles of Fat1 in controlling mitochondrial function and cell growth [12], transcriptional regulator HHEX [13], and FOXOs/sirtuins angiogenesis [14, 15] in vascular aging and conducted extensive research to understand heart diseases including vascular dysfunction. With the

development of high-throughput microarray technology, gene expression profiles have been used to identify genes and pathways associated with the pathogenesis of vascular aging, which has helped to partially illustrate the underlying mechanisms. For example, two transcriptomic studies identified some differentially expressed genes related to age-related vascular changes based on gene expression profiling in mice [16, 17]. However, these studies put emphasis only on screening differentially expressed genes (DEGs) rather than determining the connection between them, in which genes with similar expression patterns may be functionally related. Moreover, the regulatory interactions between genes in particular pathways or biological processes across multiple vascular aging stages have not been investigated. Additionally, potential novel regulators of transcription and post-transcription of age-related vascular gene expression, including micro-RNAs, long noncoding RNAs, and transcription factors, have not been investigated how they regulate the transcription-level mRNA interactions. Gene interactions in vascular aging lead to endothelial cell metabolism, thereby understanding the functional molecular mechanisms regulated by these interactions is essential for gaining biological insights into cellular functions, predicting downstream events, and ideally manipulating the aging process based on desired goals. Co-expression network analysis enables us to cluster genes by assigning them to known biological functions in which they are involved [18]. Among the co-expression network inference algorithms, weighted gene co-expression network analysis (WGCNA) is a relatively new statistical method not only to infer correlation pattern between two genes but also covers neighborhood across expression data [19] while constructed networks generally could be divided to modules. Plenty of evidence suggested the modules as stable units underlying transcriptional regulation networks whose function can remain the same while individual gene expression can be changed

or replaced by other genes with similar redundant functions [20].

In this study, we conducted a co-expression network analysis for identifying putative genes and pathways involved in a triangle of aging, vascular dysfunction, and lipid levels. A network-driven integrative analysis was performed to find significant modules and module preservation test was conducted to test the robustness of the significant modules. Further gene ontology and protein-protein interaction analyses were conducted to determine potential biomarkers in the progress of vascular aging with wet-lab verifications. Through co-expression network analysis adopted by WGCNA, we identified triglyceride-related traits correlated with gene expression changes in mouse aorta controlled by aging. Functional analysis of the top modules implies a relationship between aging-related transcriptional changes and fat components in aorta.

## RESULTS

### Network construction and module detection

After microarray data preprocessing, a total of 2,256 differentially expressed Agilent transcripts were left. We further removed ambiguous probes and duplicated genes. The ambiguous probes included positive and negative controls in the microarray, and the duplicated genes were removed according to their gene symbols. Finally, the expression values of the 469 differential genes were selected for subsequent analysis. In graph theory, the nodes with higher connections are more likely to be pivotal connectors. Likewise, critical points controlling important dynamic components in biological networks [21], removal of them may cause biological systems failure in saving their coherence. In order to identify such interconnected genes from aging-associated co-expression network abstractly, adjacency matrix was obtained from the Pearson correlation matrix with a power  $\beta=12$  based on the scale-free topology criterion [21]. Subsequently, the represented matrix was transformed to similarity matrix in clustering process during which genes grouped in a cluster were likely to be biologically relevant to the same pathway. The value of power  $\beta=12$  could emphasize robust correlations and remove unreliable correlations between genes on an exponential level. Figure 1A shows the determination of  $\beta$  parameter based on the description in the WGCNA manual. Briefly, given Agilent series GSE50833, we used the WGCNA to establish a number of modules in co-expression network, and 6 modules were obtained (Figure 1B). As illustrated in Figure 1B, modules in gene dendrogram are shown in different colors and based on dynamic branch cutting algorithm underneath row color assigns the modules membership.

### Modules associated with vascular aging and lipid levels

We aimed to gain new insights into the roles of specific modules that might be involved in vascular aging, module eigengenes associated with phenotypic traits were assessed in this study. An eigengene is referred to as gene expression profiles inside each of the modules summarized by the first principle component. The turquoise and blue modules that are positively correlated with triglyceride, leptin, and free fatty acid (FFA) respectively, were established to be significantly associated to vascular aging stage with an absolute correlation coefficient of  $>0.6$  and p-value of  $<0.05$ . Figure 2A shows a highly significant correlation between gene significant (GS) versus module membership (MM) in the turquoise module with Triglyceride, and Figure 2B illustrates the correlation between turquoise module size and triglyceride. Next, we examined whether significant modules (turquoise and blue) were enriched for GO terms relevant to age-related vascular disorders. Gene ontology enrichment analysis for the turquoise module is presented in Table 1 and the GO analysis of other modules are presented in Supplementary Table 5. From Table 1, we noticed that 44 genes are involved in the proteolysis biological process, and the products of 46 genes are located under membrane-bounded vesicle.

### Inference of miRNA–mRNA–transcription factor interaction

The top 30 interconnected genes within each of the turquoise, blue and red modules were graphically depicted by utilizing Cytoscape (Supplementary Tables 17, 19, 21). Interestingly, miRNA-target analysis showed that in the turquoise module, gene F3 is putatively targeted by 23 and 38 predicted miRNAs from TargetScan and MicroCosm respectively (Figure 3A). Additionally, in the blue module, gene H2-Q7 illustrated to be targeted by 78 miRNAs in MicroCosm (Figure 3B). No genes were found to be targeted with miRNAs in the red module. Among the miRNAs, mmu-miR-449a, mmu-miR-449c, mmu-miR-34c, mmu-miR-34b-5p, mmu-miR-15a, and mmu-let-7 were listed as common between networks built by turquoise and blue modules. Due to the inconvenience of considering a highly dimensional set of transcription factors, we only investigated transcription factors in a network of the top 90 connected hub nodes depicted for mRNA-miRNA interaction analysis (Supplementary Table 9), when transcription factors Pax8 and Hsf1 were ranked as the most significant based on the normalized enrichment score test (NES) (Table 2).

### Module preservation test

To test if the age-dependent modules are preserved between the constructed network and a reference

network, we built a reference network based on 1036 significantly differentially expressed transcripts with  $P < 0.05$  from 6-month old wild-type mice ( $n=3$ ) and 20-month old wild-type mice ( $n=3$ ) in the GSE10000 dataset (Supplementary Table 3). Among the 2,256 transcripts from GSE50833 datasets, 125 genes (according to the gene symbols) were matched with modules defined by Ghazalpour et al. [22] (Supplementary Table 4), by which we had already built a reference network. Median rank and Z-summary values were calculated to conduct module preservation test, and both measures revealed high preservation of green and blue modules between the two networks (Supplementary Figure 5A and 5B). Largely overlapped interactions between the two networks were found in this study,

indicating the robustness of the built modules is strong. The strong module preservation could be due to the overlapped interactions between the two networks, which indicate that the gene interactions within a module are conserved.

### qPCR validation of the key genes

To verify the main conclusion drawn from the microarray results, the relative expression levels of the five key genes (Enpp5, Fez1, Kif1a, F3, and H2-Q7) and their interacting microRNAs (mmu-miR-449a, mmu-miR-449c, mmu-miR-34c, mmu-miR-34b-5p, mmu-miR-15a, and mmu-let-7) were determined using qPCR. No significant difference in body weight was detected

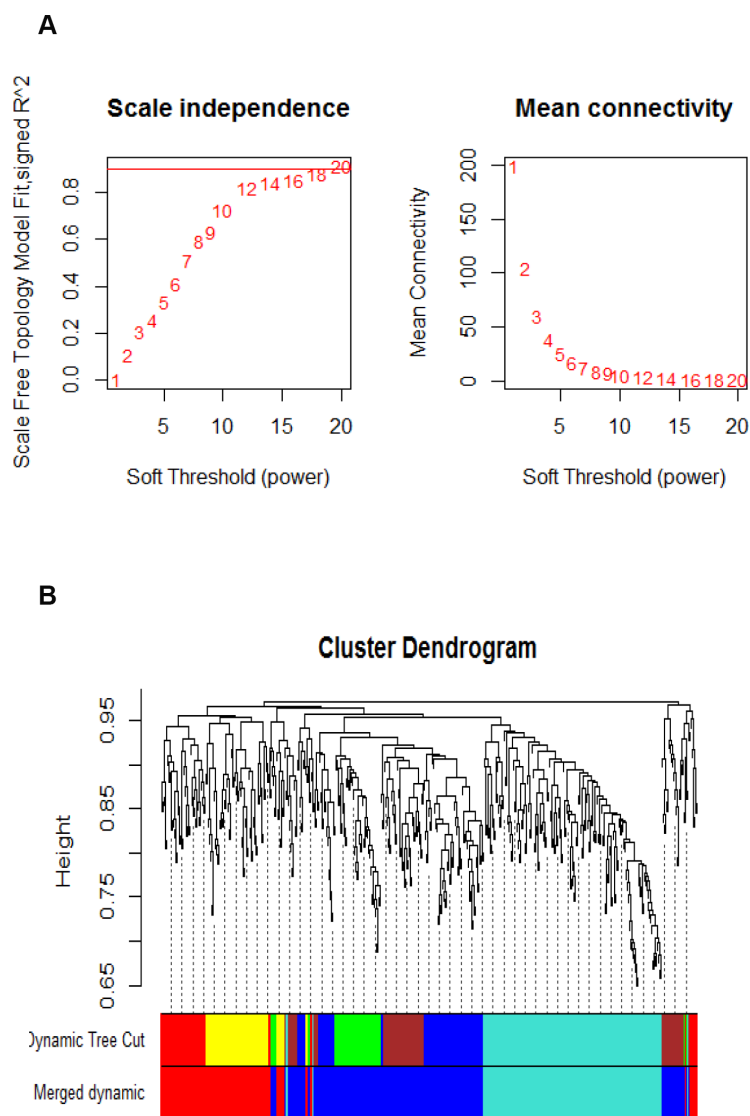


**Figure 1. Parameter analysis of inferred co-expression network and modules.** (A) A scaling factor beta determination based on the scale-free topology criterion. (B) Hierarchical clustering of genes in significant modules. The colors are assigned to each module by the Dynamic Tree Cut algorithm.

between the two groups of male mice. The RT-qPCR analysis results indicated that *Enpp5*, *Fez1*, *Kif1a*, *F3*, *mmu-miR-34c*, *mmu-miR-34b-5p*, and *mmu-let-7* were significantly up-regulated in samples from 20-month old mice group compared with the 6-month old mice group, whereas *mmu-miR-449a* and *mmu-miR-449c* were significantly down-regulated. Meanwhile, there were no significant differences observed in the *H2-Q7* and *mmu-miR-15a* genes between the two groups, but the expression level of *H2-Q7* is a little higher in the group of old mice compared to the young mice.

## DISCUSSION

The purpose of this investigation was to identify fundamental mechanisms leading to transcriptional changes in mouse aorta toward aging with a network biology approach. Given the most variable transcripts in aorta between 6-month old mice (n=6) and 20-month old mice (n=6) as a discovery dataset, we built a weighted co-expression network. This network-based approach summarizes genes with similar expression profiles into the same modules, and therefore, co-grouped genes

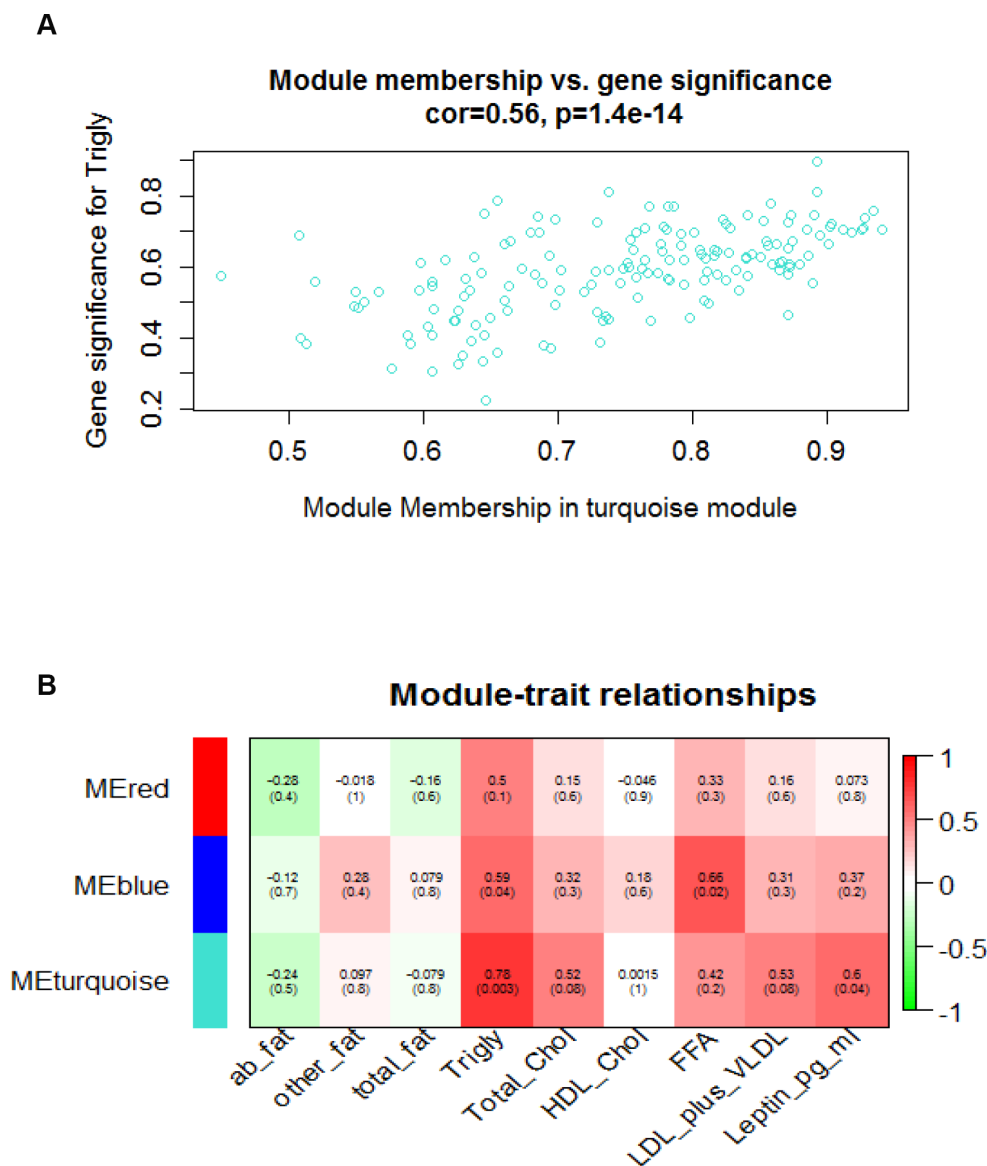


**Figure 2. Module-traits and module\_membership-gene\_significance correlation analyses.** (A) Scatterplot shows a highly significant correlation between gene significant (GS) versus module membership (MM) in the turquoise module with Triglyceride. (B) Heatmap shows correlation between assayed traits and module eigengene values. Green and red colors represent the negative and positive correlation respectively. Decimals outside of round brackets are correlation, and decimals inside of round brackets stand for gene significance level.



**Table 1. GO enrichment analysis of genes assigned to the turquoise module.**

Category	Term	Counts of genes	P-value
CC	extracellular matrix	16	0.000855
CC	mitochondrial envelope	10	0.0017607
CC	mitochondrial membrane	10	0.0017607
CC	neuron projection	23	0.0048588
BP	Proteolysis	24	0.0061265
CC	neuron part	26	0.0064492
BP	Circulatory system process	14	0.0065327
BP	Blood circulation	14	0.0065327
CC	Membrane-bounded vesicle	45	0.0072194
CC	Organelle inner membrane	6	0.0074282

BP: biological process; CC: cellular component

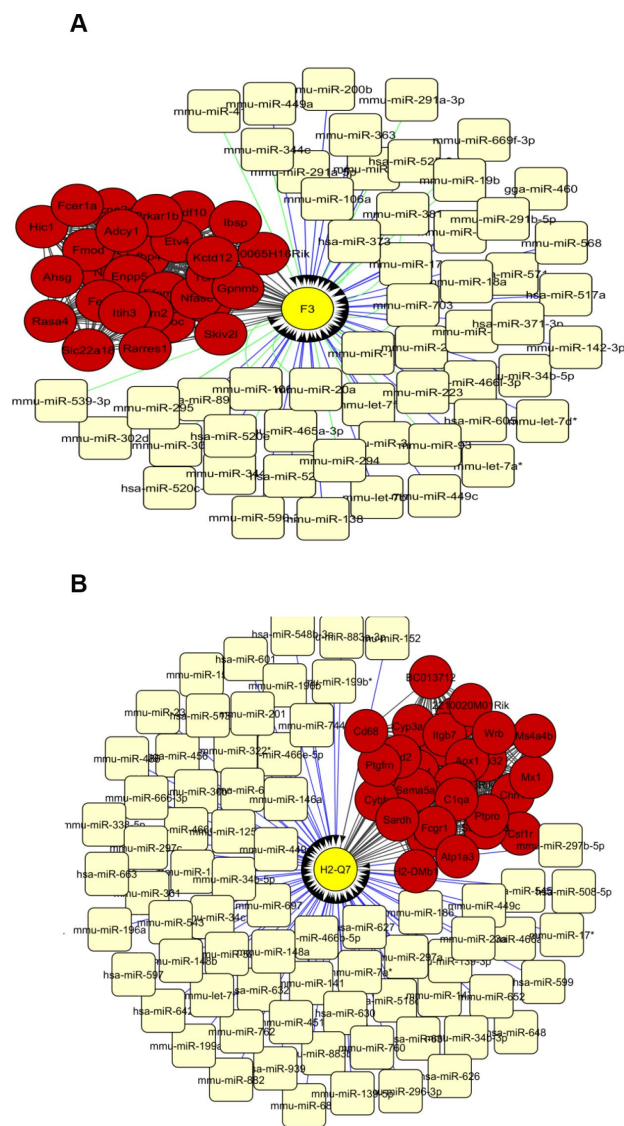


**Figure 3.** The network of top 30 interconnected genes in the turquoise (A) and blue (B) modules and predicted miRNAs from TargetScan and Microcosm. The hub genes are shown in red and miRNAs in light yellow. mRNA-miRNA interactions from TargetScan and Microcosm are shown in green and blue lines respectively. Yellow circles show the genes that are putatively regulated by miRNAs.

**Table 2. Promoter analysis of the top 90 hub genes obtained from three modules significant associated with vascular aging status.**

Transcription factor	NES	No. of targets	No. o Motifs/Tracks
Pax8	4.484	25	7
Hsf1	4.04	11	1
Pou5f1	3.916	27	2
Ovol1	3.78	14	3
Lef1	3.589	12	4
Zic2	3.485	17	2
Rfx2	3.464	6	3
Egr1	3.433	14	3
Gata2	3.422	12	1
Gltpd1	3.287	11	2
Hic1	3.224	11	3
Zfat	3.212	22	3
Sod1	3.14	4	1
Irf4	3.047	10	1
Mtf1	3.034	11	2

NES: normalized enrichment score

are thought to be involved in the same regulatory pathways [23]. When employing the Dynamic Tree Cut method, we detected 6 modules ranging from 160 genes in the turquoise module to 50 genes in the red and green modules. After merging modules with highly correlated eigengenes, the turquoise, blue and red modules were chosen for subsequently functional analysis (Supplementary Figures 1–4). To reveal vascular transcriptome’s relationship to age, we further detected trait-related gene modules and hub genes by incorporating lipid-related traits, such as triglycerides and free fatty acid, into the network analysis. Modules that are closely associated with clinical traits, might be biologically important in bridging aging and the incidence of vascular disorders. Therefore, it could draw an interaction between these traits and variable aging-associated gene expression changes in mouse aorta. The red module showed no correlation with assayed traits while the most significant and correlated module with the incorporated traits was turquoise (Figure 2, Supplementary Figure 7 and Supplementary Table 11).

Functional enrichment analysis of this module with DAVID software identified several terms apparently associated with aging-related vascular dysfunction, including extracellular matrix, blood circulation, circulatory system process, and proteolysis. Ponticos M et al. reported the cross-talk between extracellular matrix and vascular disorders in detail [24]. Blood vessels are distended by blood pressure and, therefore, require ECM

components with elasticity yet with enough tensile strength to resist rupture and stiffness.

Our clinical implication of significant modules indicated that triglyceride and leptin levels are correlated with the turquoise module, and triglyceride and free fatty acid (FFA) levels are correlated with blue module, respectively. Whereas the correlation between triglyceride level with turquoise module was higher than that with blue module (Supplementary Figure 6 and Supplementary Table 11). Noblet et al. suggested that leptin is a key modulator in pathways involved in vascular proliferation [25]. Additionally, leptin sensitivity pointed to be declined during aging in rodents [26]. People found that hypertriglyceridemia may act as a prevalent risk factor for cardiovascular disease [27] and free fatty acid level may increase with aging [28].

Through module preservation analysis, our findings were strongly validated in the blue and green modules in an independent reference network, and the blue module was more preserved between the two networks and enriched with genes involved in immune response, leukocyte differentiation and hemopoiesis. In concordance, the study from Stervbo U et al. [29]. demonstrated that age-dependent detrimental alterations in leukocytes may dysfunction the innate immune system. Additionally, Babio N et al. [30] disclosed an association between leukocyte counts with hypertriglyceridemia. The free fatty acid may activate leukocytes following endothelial dysfunction through enhanced angiotensin II production [31].

The WGCNA package also computed two values as gene significance (GS) and module membership (MM) when the smaller corresponding p-value denotes higher Pearson’s correlation coefficient between gene expression profiles, incorporated clinical traits and modules, respectively (2) and candidate mRNAs with the highest GS and MM could be considered as the one significantly associated with phenotypic trait and module eigengene of a given module (Supplementary Tables 10–12). Hereby we focused on the turquoise module, the most correlated with triglyceride level. The top 13 genes with higher MM and GS were selected as the most biologically correlated with triglyceride level and turquoise module respectively (Table 3). Consequently, Fez1, Kif1a, and Enpp5 were interesting genes as they were common among the top 30 connected genes visualized by Cytoscape (Figure 2B) and highly ranked genes based on GS and MM scores. Fez1 encodes an elongation protein that abnormally aggregated in aged mice [32]. Kif1a was exhibited as a crucial regulator of synaptic aging [33]. These highly connected inter-modular genes can be considered hubs and likely to play pivotal roles in maintaining the network functions.

**Table 3. List of genes most correlated with triglyceride and turquoise module eigengene.**

Gene	P-value (GS)	Gene	P-value (MM)
<i>Enpp5</i>	7.51E-05	<i>Igfbp4</i>	5.11E-06
<i>Fez1</i>	0.0013665	<i>Kif1a</i>	8.62E-06
<i>Il3ra</i>	0.0013893	<i>Rasa4</i>	1.32E-05
<i>Slc6a15</i>	0.0024338	<i>Skiv2l</i>	1.44E-05
<i>Igfbp2</i>	0.0029863	<i>Myoc</i>	1.51E-05
<i>Ache</i>	0.0032684	<i>Nfasc</i>	2.42E-05
<i>Spry1</i>	0.003308	<i>Kctd12</i>	3.55E-05
<i>Crfl1</i>	0.0033796	<i>Slc22a18</i>	5.59E-05
<i>Kif1a</i>	0.0042745	<i>Ibsp</i>	5.98E-05
<i>Ier3</i>	0.0049655	<i>Hic1</i>	6.21E-05
<i>Etv4</i>	0.0054145	<i>Prkar1b</i>	8.48E-05
<i>F3</i>	0.005536	<i>Fez1</i>	9.26E-05
<i>Mbd2</i>	0.005852	<i>Enpp5</i>	9.31E-05

GS: gene significance, MM: module membership

Centrality analysis of genes within turquoise and blue modules (Supplementary Tables 13–14) by use of CytoNCA [34] revealed that *Enpp5* had the highest between-centrality among the first 30 genes (Supplementary Table 15). *Enpp5* is known to have catalytic activity, and its expression is changed in adipocytes transfected with *Agt*-shRNA, indicating that this gene is involved in blood pressure and lipid accumulation [35]. String protein-protein interaction networks of *Enpp5* was presented in Supplementary Figure 8. It was also shown that *Enpp5* acts as an extracellular signaling molecule in a broad variety of tissues [36]. In a word, lipid components, including triglyceride and free fatty acid, may inhibit the activities of blood cells to cause plying in immune system following by vascular endothelial disruption. According to the GO analysis, genes *F3*, *H2-Q7* and *Enpp5* are therefore considered to be key genetic elements in age-related vascular changes. *F3* is related to angiogenesis and coagulation cascades and was suggested to be involved in pathways that are relevant to apoptosis in aging mice [37]. *H2-Q7* is a murine nonclassical MHC class I gene involved in the modulation of immune responses, whose expression showed gradual increase with aging [38]. The differential expression of *H2-Q7* may contribute to the distinct patterns of mouse susceptibility/resistance to infectious and noninfectious disorders. In a recent study [39], miRNA families *mir-34*, *mir-15* and *mir-449* exhibited significant distinct expression patterns along with aging in mice. The levels of *miR-34c* are elevated in the hippocampus of AD patients and corresponding mouse models [40]. Guo et al. demonstrated kallistatin may reduce vascular aging by

regulating microRNA-34a-SIRT1 pathway [41]. miRNA *let-7* plays a role in tissue homeostasis, repair, and stem cell aging [42].

The key genes identified through our co-expression network are concordant with other aging-related findings. The availability of massive transcriptomic data has facilitated the reconstruction of biological networks, through which we are able to decipher how genes are interacted within intricate networks underlying age-related vascular disorders. We noted that, in agreement with previous significant experimental confirmation, network mining is robust to identify hub genes and depict the structural and functional features of biological networks. Compared to methods solely based on single genes derived by differential expression analysis, biological modules may represent more credible information. In frame of accurate approaches of network reconstruction and modularity analysis, we identified the hub genes *Enpp5*, *Fez1*, *Kif1a*, *F3*, *H2-Q7*, two transcription factors *Pax8* and *Hfs1*, and their interacting miRNAs *mmu-miR-449a*, *mmu-miR-449c*, *mmu-miR-34c*, *mmu-miR-34b-5p*, *mmu-miR-15a*, and *mmu-let-7*, whose interactions could lead to age-related vascular dysfunctions.

Transcriptional alterations of the hub genes *Enpp5*, *Fez1*, *Kif1a*, and *F3*, and the interacting microRNAs *mmu-miR-34c*, *mmu-miR-34b-5p*, *mmu-let-7*, *mmu-miR-449a*, and *mmu-miR-449c* between 20 pairs of 6-month and 20-month old mice were confirmed by RT-PCR in our separate investigation. Whereas, no significant differences were observed in the *H2-Q7* and *mmu-miR-15a* genes between the two groups, even though the expression level of *H2-Q7* is a little higher in the group of old mice compared to the young mice, which may be due to the limited sample size.

We still need to be cautious to understand the biological network related to vascular aging in mice. First, the small sample size limited the findings and the results would be more reliable when utilizing a more adequate number of samples. Second, network analysis at transcriptome level could be more intensified through merging studies with entire protein-protein network to draw more precise conclusions regarding predicted hub genes and master regulators. Finally, we inferred an undirected network in which connectivity between nodes does not indicate the causal regulatory relationships.

In conclusion, triglyceride, free fatty acid, and leptin were significantly and positively correlated with age-related transcriptional changes in mice aorta. Meanwhile, five hub genes *Enpp5*, *Fez1*, *Kif1a*, *F3*, *H2-Q7*, two transcription factors *Pax8* and *Hfs1*, and their interacting miRNAs *mmu-miR-449a*, *mmu-miR-449c*, *mmu-miR-34c*, *mmu-miR-34b-5p*, *mmu-miR-15a*, and *mmu-let-7*



exhibited the most connectivity with external lipid-related traits, and their interactions could lead to age-related vascular dysfunctions. Transcriptional alterations were confirmed with RT-PCR for the hub genes *Enpp5*, *Fez1*, *Kif1a*, and *F3*, and the interacting microRNAs *mmu-miR-34c*, *mmu-miR-34b-5p*, *mmu-let-7*, *mmu-miR-449a*, and *mmu-miR-449c*, which could serve as potential biomarkers in vascular aging.

## MATERIALS AND METHODS

### Data collection

We carefully selected vascular aging-associated dataset from the National Center for Biotechnology Information (NCBI) Gene Expression Omnibus (GEO, <http://www.ncbi.nlm.nih.gov/geo/>) database, and identified two time-series microarray datasets regarding vascular aging in mice aorta (GEO access number: GSE50833; GSE10000). The Agilent TXT files for GSE50833 and Affymetrix TXT files for GSE10000 were downloaded from the GEO database respectively. The data GSE50833 [16] was used as first-stage discovery set for co-expression network construction, and GSE10000 [17] as a second-stage independent verification dataset for module preservation test. This dataset GSE50833 consists of a total of 12 samples with data generation platform of GPL10787, and these samples correspond to 6-month old mice (n=6) and 20-month old mice (n=6). The data GSE10000 consists of a total of 18 samples with data generation platform of GPL1261 and GPL8321 respectively, and these samples correspond to three pairs of 6-week old wild-type and *ApoE*<sup>-/-</sup> mice, three pairs of 32-week old wild-type and *ApoE*<sup>-/-</sup> mice, and three pairs of 78-week old wild-type and *ApoE*<sup>-/-</sup> mice.

### Data preprocessing and identification of DEGs

Statistical software R (version 3.5.1) and its related packages were used for data preprocessing and identifying nominal DEGs between the two aging stages. The *affyPLM* package could fit the original data of the microarray to generate the weights and residuals diagram, the relative log expression (RLE), and the relative standard deviation (NUSE, Normalized unscaled standard errors) box diagram. Before we analyzed the data, we conducted quality testing of microarray data. In this process, we used some powerful and accurate R packages, such as *affyPLM*, *affy*, and *RColorBrewer*. After conducting the procedure of removing unqualified samples or probes, we got a reasonable and useful sample set. Raw files were normalized with quantile method (Supplementary Table 1) and the *limma* package (Linear Model for Microarray Data) was applied to extract genes with  $P < 0.05$  by comparing the gene expression values between the 6- and 20-month old mice. These genes were

considered as nominal DEGs without multiple test correction. Ultimately, the extracted Agilent probe IDs of the identified DEGs for the data GSE50833 were transformed into Agilent MIT IDs (Supplementary Table 2) and used for follow-up analysis.

### Network construction

After removing the redundant probes that were not able to contribute greatly to the construction of modules, the nominal DEGs were used to build weighted gene co-expression network through the WGCNA R package, by which the calculated absolute value of the Pearson correlation coefficient for all pair-wise comparisons of gene expression values was transformed into a similarity matrix. Next, the similarity matrix was applied to *stepBystep*, a network construction, and module detection function. We carried out this step by building a weighted matrix with a scaling factor-beta based on the assumption that biological networks are scale-free [43]. The modules were computed by assigning a minimum of 30 genes per module and keeping the default value of *SplitDepth* in two for a medium sensitivity of cluster splitting. These parameters would optimize scale-free topology and robust node connectivity criteria when any two genes were connected, and the edge weight was determined by the topological overlap matrix (TOM). Furthermore, genes were clustered into modules by utilizing average linkage hierarchical clustering using topological overlap dissimilarity matrix (1-TOM) as the distance measure, and modules were determined by the dynamic hybrid tree cut algorithm. Finally, similar modules whose eigengenes were highly correlated were merged to trim genes whose correlation with module eigengene was less than the defined threshold (hereby we used 0.25 as a threshold for merging similar modules). WGCNA determines highly inter-connected nodes as modules designated with different colors. Moreover, this algorithm is able to relate the identified modules to external clinical outcomes, and to export the network information to external software for visualization, e.g. *VisANT* (<http://visant.bu.edu/>) [44] or *Cytoscape* [45] that visualizes biological interactions between subnetworks.

### Gene ontology analysis and visualization

Gene Ontology (GO) analysis was conducted to reveal biological functions of gene products within significant modules from three scenarios: biological process (BP), cellular component (CC), and molecular function (MF) by using the software named Database for Annotation, Visualization, and Integrated Discovery (DAVID) [46]. DAVID facilitates high throughput gene functional analysis by accepting the input of a list of genes or an individual gene. Potential enriched functions of the

DEGs in the determined modules were analyzed by the DAVID tool.

The top 30 high-rank intramedullary hub genes were prepared for visualization with VisANT (Supplementary Tables 16–21).

### Modeling miRNA–mRNA–transcription factor interaction

To explore transcription factor and miRNA–mRNA interaction in particular modules, the database TargetScan Mouse (Release 7.1) ([http://www.targetscan.org/vert\\_71/](http://www.targetscan.org/vert_71/)) was used for searching the predicted microRNA targets, and MicroCosm Mouse (Release 5) (<http://www.ebi.ac.uk/enright-srv/microcosm/htdocs/targets/v5/>) was used to build a miRNA–mRNA interaction network and the network was visualized with Cytoscape 3.3.8 software [46]. Putative miRNAs were generated by the intersection of the miRNA–targets from TargetScan and Microcosm. Transcription factors may control different gene modules. Therefore, we further used iRegulon Cytoscape plugin [47] to identify the possible transcription factors and their co-factors that are associated with a collection of intramedullary hub genes extracted from prognosticate modules (Supplementary Tables 6–9). To expand our network, we employed CyTargetLinker plugin [48]. CyTargetLinker is able to enhance biological networks using the provided information in frame of Regulatory Interaction Networks or RegIN. RegIN is a network in xgmml format containing regulatory interactions.

### Module preservation

To determine the reliability of the identified vascular aging-related modules and compare the modular structure in inferred co-expression network with a reference network generated based on an independent dataset, we used a previous study with GEO access number GSE10000 [17] to identify significantly differentially expressed genes ( $P < 0.05$ ). In the dataset GSE10000, the two groups of samples corresponding to 32-week old wild-type mice (around 6-month old) ( $n=3$ ) and 78-week old wild-type mice (around 20-month old) ( $n=3$ ), were comparable with the first-stage samples corresponding to 6-month old mice ( $n=6$ ) and 20-month old mice ( $n=6$ ). Therefore, we removed the samples corresponding to 6-week old mice ( $n=3$ ) and the ApoE<sup>-/-</sup> mice. Based on the significantly differentially expressed probe sets, we reconstructed a test co-expression network and contrasted the preservation of co-expression network across testing and reference datasets to detect the conservation of gene pairs between the two networks. Briefly, a Z-summary  $< 5$  and lower median rank indicates weak preservation between the testing and reference networks.

### Animal breeding, mouse aorta isolation, and real-time polymerase chain reaction

All animal experiments were approved by the Animal Ethics Committee of Shanghai Jiao Tong University. Male mice (C57BL/6J) were obtained from the Shanghai Laboratory Animal Center, Chinese Academy of Sciences (SLAC, CAS), and kept for 7 days in the local animal house for acclimatization. The mice were 6 and 20 months of age old, housed at a constant ambient temperature under a 12h/12h light-dark cycle and supplied with distilled water, and pelleted AIN-76A (Research Diets, New Brunswick, NJ) chow ad libitum. Quantitative real-time polymerase chain reaction (qPCR) was used to validate the expression of genes changed in aortas from mice aged 6-month ( $n = 20$ ) and 20-month ( $n = 20$ ).

A mouse aorta was perfused in situ with cautious to keep the adventitia intact. The vessel was flushed thoroughly with ice-cold phosphate-buffered saline (PBS), through the left ventricle of the heart, cleaned periadventitial fat and connective tissues, snap-frozen in liquid nitrogen, and stored at  $-80^{\circ}\text{C}$ .

Total RNA, including miRNA, was extracted from the tissue using Qiagen RNeasy Mini Kit (Qiagen, Hilden, Germany). Total RNA from aorta was treated with DNase I to remove genomic DNA. RNA integrity was checked by Agilent2100 Bioanalyzer (Agilent Technologies, Palo Alto, CA) and RNA gel electrophoresis.

For the quantification of mRNAs, 1  $\mu\text{g}$  of the total RNA was converted into cDNA using a reverse transcription kit (Promega) based on the manufacturer's instruction. The gene expression of hub genes (Enpp5, Fez1, Kif1a, F3, and H2-Q7) were then detected by real-time qPCR. The qPCR were conducted using SYBR Premix Ex Taq (Takara, Japan) in 20  $\mu\text{l}$  reaction solution containing 1  $\mu\text{l}$  cDNA, 10  $\mu\text{l}$  SYBR Premix Ex Taq (2X), 0.4  $\mu\text{l}$  forward primer, 0.4  $\mu\text{l}$  reverse primer, 0.4  $\mu\text{l}$  ROX reference dye, and 7.8  $\mu\text{l}$  ddH<sub>2</sub>O. The PCR amplification procedure was carried out on an ABI 7500 fast real-time PCR system (Applied Biosystems, USA) at  $95^{\circ}\text{C}$  for 10 s, followed by 40 cycles of  $95^{\circ}\text{C}$  for 5 s and  $60^{\circ}\text{C}$  for 35 s. The amplification reaction without the template was used as a negative control.  $\beta$ -actin gene was used as the internal reference. Primers used for gene amplification are available on request.

The miRNAs (mmu-miR-449a, mmu-miR-449c, mmu-miR-34c, mmu-miR-34b-5p, mmu-miR-15a, and mmu-let-7) were detected by qPCR. Briefly, 2  $\mu\text{g}$  RNA were performed using the miRcute miRNA First-Strand cDNA Synthesis Kit (Tiangen, Beijing, China). The qPCR was then conducted using the miRcute miRNA qPCR Detection Kit (SYBR) (Tiangen, Beijing, China)

in 20  $\mu$ l reaction solution containing 1  $\mu$ l cDNA, 10  $\mu$ l 2 $\times$  miRcute miRNA premix, 0.4  $\mu$ l 50 $\times$  ROX Reference Dye, 0.4  $\mu$ l forward primer, 0.4  $\mu$ l reverse primer, and 7.8  $\mu$ l ddH<sub>2</sub>O. The PCR amplification procedure was carried out on an ABI Prism 7500 Fast Sequence Detection System (ABI, Carlsbad, CA, USA) at 94°C for 2 min, followed by 40 cycles of 95°C for 20 s and 60°C for 35 s. Small nucleolar RNA (RNU6B) was used as the housekeeping loading reference. Forward primers were designed based on mature miRNA sequences while the reverse primers were provided by the miRcute miRNA qPCR Detection Kit (SYBR) (Tiangen, Beijing, China).

The relative gene expression was calculated using the 2<sup>- $\Delta\Delta$ Ct</sup> method [49] (Song et al., 2018). The experiments were conducted three times independently. Statistical comparison of the levels was analyzed using two-tail unpaired Student's t-test, and differences were considered significant if  $P < 0.05$ .

## AUTHOR CONTRIBUTIONS

MX designed the research. MX XW, HL, and XL performed the experiments and/or data analysis. SD, XLT, and QL helped to perform the validation experiments. MX, XLT, and GA drafted the manuscript, and all authors revised the paper.

## ACKNOWLEDGMENTS

We are grateful for the suggestive comments from Dr. Kai Wang from Shanghai Jiao Tong University affiliated Shanghai Chest Hospital.

## CONFLICTS OF INTEREST

The authors of this manuscript have no conflict of interest to declare.

## FUNDING

We acknowledge financial support by the National Key Basic Research Program of China (2013CB530700), Shanghai Municipal Commission of Science and Technology Program (13JC1403700), “Eastern Scholar” project supported by Shanghai Municipal Education Commission (No. ZXDF089002), Shanghai Key Laboratory of Psychotic Disorders (13dz2260500, 14-K06), and National Natural Science Foundation of China (81630034), and K. C. Wong Magna Fund in Ningbo University.

## REFERENCES

1. Lakatta EG, Levy D. Arterial and cardiac aging: major shareholders in cardiovascular disease enterprises: Part I: aging arteries: a “set up” for vascular disease. *Circulation*. 2003; 107:139–46. <https://doi.org/10.1161/01.CIR.0000048892.83521.58> PMID:[12515756](https://pubmed.ncbi.nlm.nih.gov/12515756/)
2. Lakatta EG. Arterial and cardiac aging: major shareholders in cardiovascular disease enterprises: Part III: cellular and molecular clues to heart and arterial aging. *Circulation*. 2003; 107:490–97. <https://doi.org/10.1161/01.CIR.0000048894.99865.02> PMID:[12551876](https://pubmed.ncbi.nlm.nih.gov/12551876/)
3. Ohira T, Iso H. Cardiovascular disease epidemiology in Asia: an overview. *Circ J*. 2013; 77:1646–52. <https://doi.org/10.1253/circj.CJ-13-0702> PMID:[23803294](https://pubmed.ncbi.nlm.nih.gov/23803294/)
4. Fleenor BS, Sindler AL, Eng JS, Nair DP, Dodson RB, Seals DR. Sodium nitrite de-stiffening of large elastic arteries with aging: role of normalization of advanced glycation end-products. *Exp Gerontol*. 2012; 47:588–94. <https://doi.org/10.1016/j.exger.2012.05.004> PMID:[22588062](https://pubmed.ncbi.nlm.nih.gov/22588062/)
5. Jin J, Liu Y, Huang L, Tan H. Advances in epigenetic regulation of vascular aging. *Rev Cardiovasc Med*. 2019; 20:19–25. <https://doi.org/10.31083/j.rcm.2019.01.3189> PMID:[31184092](https://pubmed.ncbi.nlm.nih.gov/31184092/)
6. Pucci G, Tarnoki AD, Medda E, Tarnoki DL, Littvay L, Maurovich-Horvat P, Jermendy AL, Godor E, Fejer B, Hernyes A, Lucatelli P, Fanelli F, Farina F, et al. Genetic and environmental determinants of longitudinal stability of arterial stiffness and wave reflection: a twin study. *J Hypertens*. 2018; 36:2316–23. <https://doi.org/10.1097/HJH.0000000000001869> PMID:[30382956](https://pubmed.ncbi.nlm.nih.gov/30382956/)
7. Jeremy RW. Calcific Aortic Valve Disease: Insights Into the Genetics of Vascular Ageing. *Circ Cardiovasc Genet*. 2017; 10:e002012. <https://doi.org/10.1161/CIRCGENETICS.117.002012> PMID:[29242202](https://pubmed.ncbi.nlm.nih.gov/29242202/)
8. Li DJ, Huang F, Ni M, Fu H, Zhang LS, Shen FM.  $\alpha$ 7 Nicotinic Acetylcholine Receptor Relieves Angiotensin II-Induced Senescence in Vascular Smooth Muscle Cells by Raising Nicotinamide Adenine Dinucleotide-Dependent SIRT1 Activity. *Arterioscler Thromb Vasc Biol*. 2016; 36:1566–76. <https://doi.org/10.1161/ATVBAHA.116.307157> PMID:[27339462](https://pubmed.ncbi.nlm.nih.gov/27339462/)
9. Sessions AO, Engler AJ. Mechanical Regulation of Cardiac Aging in Model Systems. *Circ Res*. 2016; 118:1553–62. <https://doi.org/10.1161/CIRCRESAHA.116.307472> PMID:[27174949](https://pubmed.ncbi.nlm.nih.gov/27174949/)
10. Abdellatif M, Sedej S, Carmona-Gutierrez D, Madeo F,

- Kroemer G. Autophagy in Cardiovascular Aging. *Circ Res*. 2018; 123:803–24.  
<https://doi.org/10.1161/CIRCRESAHA.118.312208>  
PMID:30355077
11. Guzik TJ, Touyz RM. Oxidative Stress, Inflammation, and Vascular Aging in Hypertension. *Hypertension*. 2017; 70:660–67.  
<https://doi.org/10.1161/HYPERTENSIONAHA.117.07802>  
PMID:28784646
  12. Cao LL, Riascos-Bernal DF, Chinnasamy P, Dunaway CM, Hou R, Pujato MA, O'Rourke BP, Miskolci V, Guo L, Hodgson L, Fiser A, Sibinga NE. Control of mitochondrial function and cell growth by the atypical cadherin Fat1. *Nature*. 2016; 539:575–78.  
<https://doi.org/10.1038/nature20170> PMID:27828948
  13. Gauvrit S, Villasenor A, Strilic B, Kitchen P, Collins MM, Marín-Juez R, Guenther S, Maischein HM, Fukuda N, Canham MA, Brickman JM, Bogue CW, Jayaraman PS, Stainier DYR. HHEX is a transcriptional regulator of the VEGFC/FLT4/PROX1 signaling axis during vascular development. *Nat Commun*. 2018; 9:2704.  
<https://doi.org/10.1038/s41467-018-05039-1>  
PMID:30006544
  14. Wilhelm K, Happel K, Eelen G, Schoors S, Oellerich MF, Lim R, Zimmermann B, Aspalter IM, Franco CA, Boettger T, Braun T, Fruttiger M, Rajewsky K, et al. FOXO1 couples metabolic activity and growth state in the vascular endothelium. *Nature*. 2016; 529:216–20.  
<https://doi.org/10.1038/nature16498> PMID:26735015
  15. Kane AE, Sinclair DA. Sirtuins and NAD<sup>+</sup> in the Development and Treatment of Metabolic and Cardiovascular Diseases. *Circ Res*. 2018; 123:868–85.  
<https://doi.org/10.1161/CIRCRESAHA.118.312498>  
PMID:30355082
  16. Rammos C, Hendgen-Cotta UB, Deenen R, Pohl J, Stock P, Hinzmann C, Kelm M, Rassaf T. Age-related vascular gene expression profiling in mice. *Mech Ageing Dev*. 2014; 135:15–23.  
<https://doi.org/10.1016/j.mad.2014.01.001>  
PMID:24447783
  17. Gräbner R, Lötzer K, Döpping S, Hildner M, Radke D, Beer M, Spanbroek R, Lippert B, Reardon CA, Getz GS, Fu YX, Hehlhans T, Mebius RE, et al. Lymphotoxin beta receptor signaling promotes tertiary lymphoid organogenesis in the aorta adventitia of aged ApoE<sup>-/-</sup> mice. *J Exp Med*. 2009; 206:233–48.  
<https://doi.org/10.1084/jem.20080752>  
PMID:19139167
  18. Khosravi P, Gazestani VH, Pirhaji L, Law B, Sadeghi M, Goliaei B, Bader GD. Inferring interaction type in gene regulatory networks using co-expression data. *Algorithms Mol Biol*. 2015; 10:23.  
<https://doi.org/10.1186/s13015-015-0054-4>  
PMID:26157474
  19. Langfelder P, Horvath S. WGCNA: an R package for weighted correlation network analysis. *BMC Bioinformatics*. 2008; 9:559.  
<https://doi.org/10.1186/1471-2105-9-559>  
PMID:19114008
  20. Chin CH, Chen SH, Wu HH, Ho CW, Ko MT, Lin CY. cytoHubba: identifying hub objects and sub-networks from complex interactome. *BMC Syst Biol*. 2014 (Suppl 4); 8:S11.  
<https://doi.org/10.1186/1752-0509-8-S4-S11>  
PMID:25521941
  21. Faith JJ, Hayete B, Thaden JT, Mogno I, Wierzbowski J, Cottarel G, Kasif S, Collins JJ, Gardner TS. Large-scale mapping and validation of Escherichia coli transcriptional regulation from a compendium of expression profiles. *PLoS Biol*. 2007; 5:e8.  
<https://doi.org/10.1371/journal.pbio.0050008>  
PMID:17214507
  22. Ghazalpour A, Doss S, Zhang B, Wang S, Plaisier C, Castellanos R, Brozell A, Schadt EE, Drake TA, Lusis AJ, Horvath S. Integrating genetic and network analysis to characterize genes related to mouse weight. *PLoS Genet*. 2006; 2:e130.  
<https://doi.org/10.1371/journal.pgen.0020130>  
PMID:16934000
  23. van Nas A, Guhathakurta D, Wang SS, Yehya N, Horvath S, Zhang B, Ingram-Drake L, Chaudhuri G, Schadt EE, Drake TA, Arnold AP, Lusis AJ. Elucidating the role of gonadal hormones in sexually dimorphic gene coexpression networks. *Endocrinology*. 2009; 150:1235–49.  
<https://doi.org/10.1210/en.2008-0563>  
PMID:18974276
  24. Ponticos M, Smith BD. Extracellular matrix synthesis in vascular disease: hypertension, and atherosclerosis. *J Biomed Res*. 2014; 28:25–39. PMID:24474961
  25. Noblet JN, Goodwill AG, Sassoon DJ, Kiel AM, Tune JD. Role of leptin in coronary vascular dysfunction and proliferation. *FASEB J*. 2016 (Suppl ); 30:733–1.
  26. Filippi BM, Lam TK. Leptin and aging. *Aging (Albany NY)*. 2014; 6:82–83.  
<https://doi.org/10.18632/aging.100637>  
PMID:24561396
  27. Kaltsas GA, Korbonits M, Isidori AM, Webb JA, Trainer PJ, Monson JP, Besser GM, Grossman AB. How common are polycystic ovaries and the polycystic ovarian syndrome in women with Cushing's syndrome? *Clin Endocrinol (Oxf)*. 2000; 53:493–500.  
<https://doi.org/10.1046/j.1365-2265.2000.01117.x>  
PMID:11012575



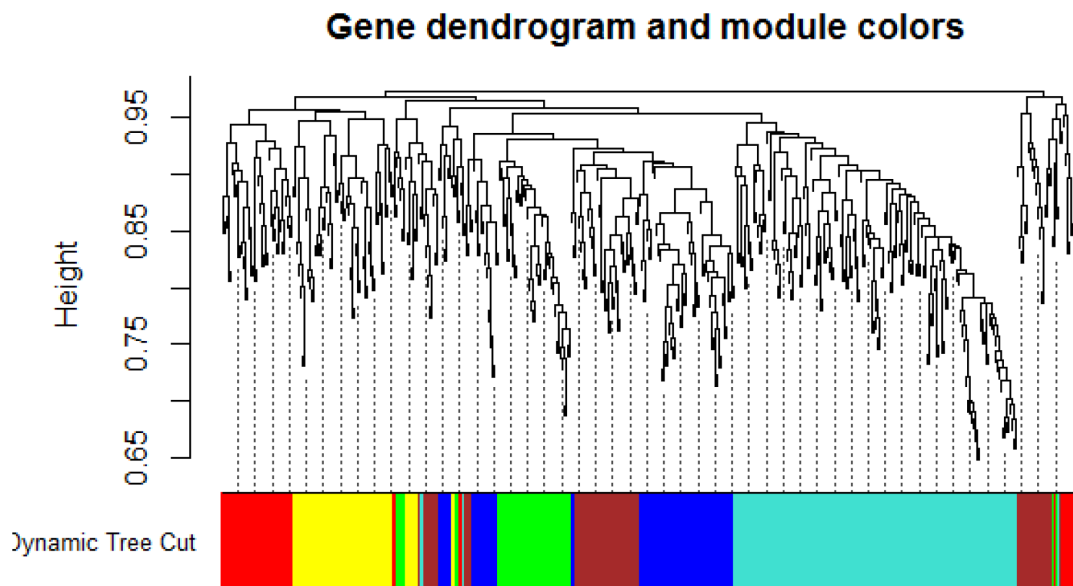
28. Talayero BG, Sacks FM. The role of triglycerides in atherosclerosis. *Curr Cardiol Rep.* 2011; 13:544–52.  
<https://doi.org/10.1007/s11886-011-0220-3>  
PMID:[21968696](https://pubmed.ncbi.nlm.nih.gov/21968696/)
29. Stervbo U, Meier S, Mälzer JN, Baron U, Bozzetti C, Jürchott K, Nienen M, Olek S, Rachwalik D, Schulz AR, Waldner JM, Neumann A, Babel N, et al. Effects of aging on human leukocytes (part I): immunophenotyping of innate immune cells. *Age (Dordr).* 2015; 37:92.  
<https://doi.org/10.1007/s11357-015-9828-3>  
PMID:[26324155](https://pubmed.ncbi.nlm.nih.gov/26324155/)
30. Babio N, Ibarrola-Jurado N, Bulló M, Martínez-González MÁ, Wärnberg J, Salaverría I, Ortega-Calvo M, Estruch R, Serra-Majem L, Covas MI, Sorli JV, Salas-Salvadó J, and PREDIMED Study Investigators. White blood cell counts as risk markers of developing metabolic syndrome and its components in the PREDIMED study. *PLoS One.* 2013; 8:e58354.  
<https://doi.org/10.1371/journal.pone.0058354>  
PMID:[23526980](https://pubmed.ncbi.nlm.nih.gov/23526980/)
31. Azekoshi Y, Yasu T, Watanabe S, Tagawa T, Abe S, Yamakawa K, Uehara Y, Momomura S, Urata H, Ueda S. Free fatty acid causes leukocyte activation and resultant endothelial dysfunction through enhanced angiotensin II production in mononuclear and polymorphonuclear cells. *Hypertension.* 2010; 56:136–42.  
<https://doi.org/10.1161/HYPERTENSIONAHA.110.153056>  
PMID:[20530293](https://pubmed.ncbi.nlm.nih.gov/20530293/)
32. Butkevich E, Härtig W, Nikolov M, Erck C, Grosche J, Urlaub H, Schmidt CF, Klopfenstein DR, Chua JJ. Phosphorylation of FEZ1 by Microtubule Affinity Regulating Kinases regulates its function in presynaptic protein trafficking. *Sci Rep.* 2016; 6:26965.  
<https://doi.org/10.1038/srep26965> PMID:[27247180](https://pubmed.ncbi.nlm.nih.gov/27247180/)
33. Li LB, Lei H, Arey RN, Li P, Liu J, Murphy CT, Xu XZ, Shen K. The Neuronal Kinesin UNC-104/KIF1A Is a Key Regulator of Synaptic Aging and Insulin Signaling-Regulated Memory. *Curr Biol.* 2016; 26:605–15.  
<https://doi.org/10.1016/j.cub.2015.12.068>  
PMID:[26877087](https://pubmed.ncbi.nlm.nih.gov/26877087/)
34. Tang Y, Li M, Wang J, Pan Y, Wu F. CytoNCA: a cytoscape plugin for centrality analysis and evaluation of biological networks. *Biosystems.* 2015; 127:67–72.  
<https://doi.org/10.1016/j.biosystems.2014.11.005>  
PMID:[25451770](https://pubmed.ncbi.nlm.nih.gov/25451770/)
35. Carroll WX, Kalupahana NS, Booker SL, Siriwardhana N, Lemieux M, Saxton AM, Moustaid-Moussa N. Angiotensinogen gene silencing reduces markers of lipid accumulation and inflammation in cultured adipocytes. *Front Endocrinol (Lausanne).* 2013; 4:10.  
<https://doi.org/10.3389/fendo.2013.00010>  
PMID:[23483012](https://pubmed.ncbi.nlm.nih.gov/23483012/)
36. Vollmayer P, Clair T, Goding JW, Sano K, Servos J, Zimmermann H. Hydrolysis of diadenosine polyphosphates by nucleotide pyrophosphatases/phosphodiesterases. *Eur J Biochem.* 2003; 270:2971–78.  
<https://doi.org/10.1046/j.1432-1033.2003.03674.x>  
PMID:[12846830](https://pubmed.ncbi.nlm.nih.gov/12846830/)
37. Puzzo D, Bizzoca A, Loreto C, Guida CA, Gulisano W, Frasca G, Bellomo M, Castorina S, Gennarini G, Palmeri A. Role of F3/contactin expression profile in synaptic plasticity and memory in aged mice. *Neurobiol Aging.* 2015; 36:1702–15.  
<https://doi.org/10.1016/j.neurobiolaging.2015.01.004>  
PMID:[25659859](https://pubmed.ncbi.nlm.nih.gov/25659859/)
38. Melo-Lima BL, Evangelista AF, de Magalhães DA, Passos GA, Moreau P, Donadi EA. Differential transcript profiles of MHC class Ib(Qa-1, Qa-2, and Qa-10) and Aire genes during the ontogeny of thymus and other tissues. *J Immunol Res.* 2014; 2014:159247.  
<https://doi.org/10.1155/2014/159247>  
PMID:[24829926](https://pubmed.ncbi.nlm.nih.gov/24829926/)
39. Victoria B, Dhahbi JM, Nunez Lopez YO, Spinel L, Atamna H, Spindler SR, Masternak MM. Circulating microRNA signature of genotype-by-age interactions in the long-lived Ames dwarf mouse. *Aging Cell.* 2015; 14:1055–66.  
<https://doi.org/10.1111/accel.12373>  
PMID:[26176567](https://pubmed.ncbi.nlm.nih.gov/26176567/)
40. Kennerdell JR, Liu N, Bonini NM. MiR-34 inhibits polycomb repressive complex 2 to modulate chaperone expression and promote healthy brain aging. *Nat Commun.* 2018; 9:4188.  
<https://doi.org/10.1038/s41467-018-06592-5>  
PMID:[30305625](https://pubmed.ncbi.nlm.nih.gov/30305625/)
41. Guo Y, Li P, Gao L, Zhang J, Yang Z, Bledsoe G, Chang E, Chao L, Chao J. Kallistatin reduces vascular senescence and aging by regulating microRNA-34a-SIRT1 pathway. *Aging Cell.* 2017; 16:837–46.  
<https://doi.org/10.1111/accel.12615> PMID:[28544111](https://pubmed.ncbi.nlm.nih.gov/28544111/)
42. Toledano H. The role of the heterochronic microRNA let-7 in the progression of aging. *Exp Gerontol.* 2013; 48:667–70.  
<https://doi.org/10.1016/j.exger.2012.08.006>  
PMID:[22960398](https://pubmed.ncbi.nlm.nih.gov/22960398/)
43. Assenov Y, Ramírez F, Schelhorn SE, Lengauer T, Albrecht M. Computing topological parameters of biological networks. *Bioinformatics.* 2008; 24:282–84.  
<https://doi.org/10.1093/bioinformatics/btm554>  
PMID:[18006545](https://pubmed.ncbi.nlm.nih.gov/18006545/)
44. Hu Z, Chang YC, Wang Y, Huang CL, Liu Y, Tian F, Granger B, Delisi C. VisANT 4.0: integrative network platform to connect genes, drugs, diseases and therapies. *Nucleic Acids Res.* 2013; 41:W225–31.



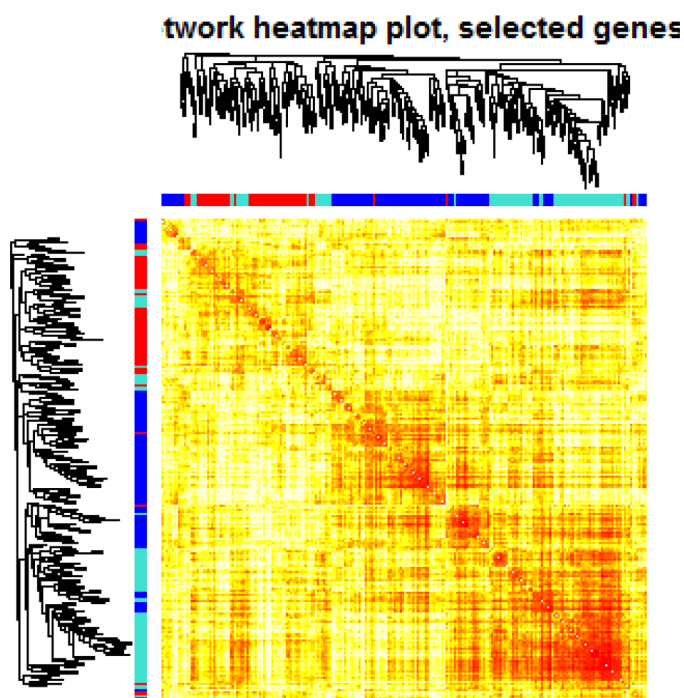
- <https://doi.org/10.1093/nar/gkt401> PMID:23716640
45. Maere S, Heymans K, Kuiper M. BiNGO: a Cytoscape plugin to assess fq of gene ontology categories in biological networks. *Bioinformatics*. 2005; 21:34489. <https://doi.org/10.1093/bioinformatics/bti551> PMID:15972284
46. Huang DW, Sherman BT, Tan Q, Kir J, Liu D, Bryant D, Guo Y, Stephens R, Baseler MW, Lane HC, Lempicki RA. DAVID Bioinformatics Resources: expanded annotation database and novel algorithms to better extract biology from large gene lists. *Nucleic Acids Res*. 2007; 35:W169–75. <https://doi.org/10.1093/nar/gkm415> PMID:17576678
47. Janky R, Verfaillie A, Imrichová H, Van de Sande B, Standaert L, Christiaens V, Hulselmans G, Herten K, Naval Sanchez M, Potier D, Svetlichnyy D, Kalender Atak Z, Fiers M, et al. iRegulon: from a gene list to a gene regulatory network using large motif and track collections. *PLoS Comput Biol*. 2014; 10:e1003731. <https://doi.org/10.1371/journal.pcbi.1003731> PMID:25058159
48. Kutmon M, Kelder T, Mandaviya P, Evelo CT, Coort SL. CyTargetLinker: a cytoscape app to integrate regulatory interactions in network analysis. *PLoS One*. 2013; 8:e82160. <https://doi.org/10.1371/journal.pone.0082160> PMID:24340000
49. Song C, Yan H, Wang H, Zhang Y, Cao H, Wan Y, Kong L, Chen S, Xu H, Pan B, Zhang J, Fan G, Xin H, et al. AQR is a novel type 2 diabetes-associated gene that regulates signaling pathways critical for glucose metabolism. *J Genet Genomics*. 2018; 45:111–20. <https://doi.org/10.1016/j.jgg.2017.11.007> PMID:29502958

## SUPPLEMENTARY MATERIALS

### Supplementary Figures

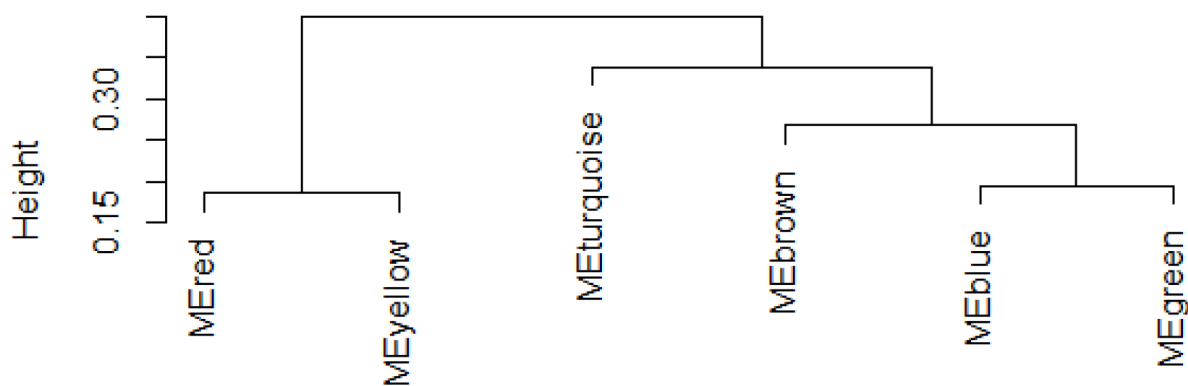


**Supplementary Figure 1. Hierarchical clustering of genes in significant modules.** The colors are assigned to each module by the Dynamic Tree Cut.

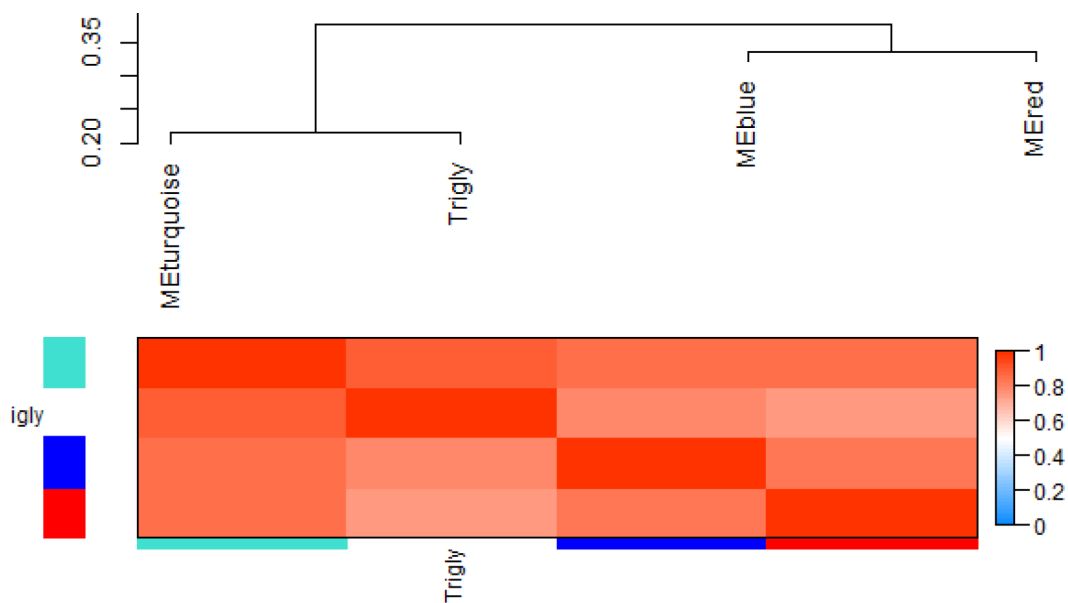


**Supplementary Figure 2. Heatmap plot of topological overlap in the gene network.** Each row and column corresponds to a gene, light color denotes low topological overlap, and progressively darker red denotes higher topological overlap. Darker squares along the diagonal correspond to modules. The gene dendrogram and module assignment are shown along the left and top.

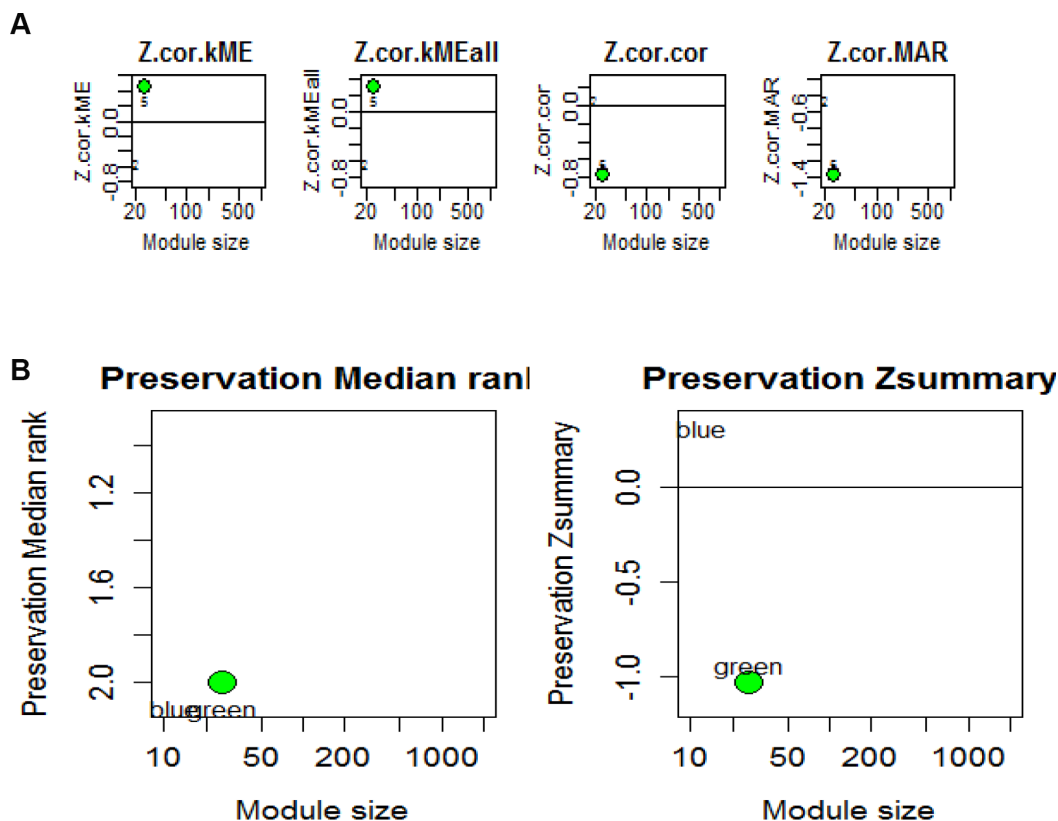
### Clustering of module eigengenes



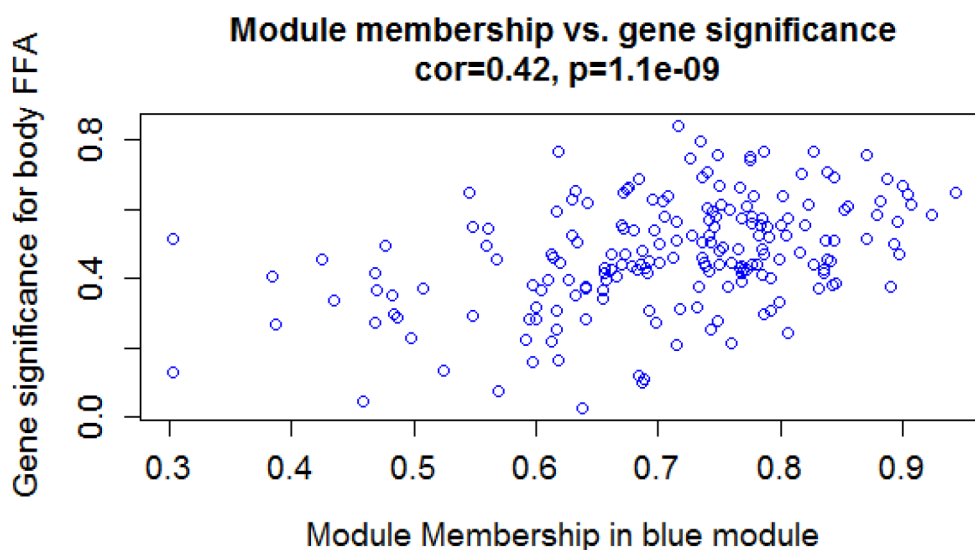
**Supplementary Figure 3. Hierarchical clustering of module eigengenes that summarize the modules found in the clustering analysis.** Branches of the dendrogram (the meta-modules) group together eigengenes that are positively correlated.



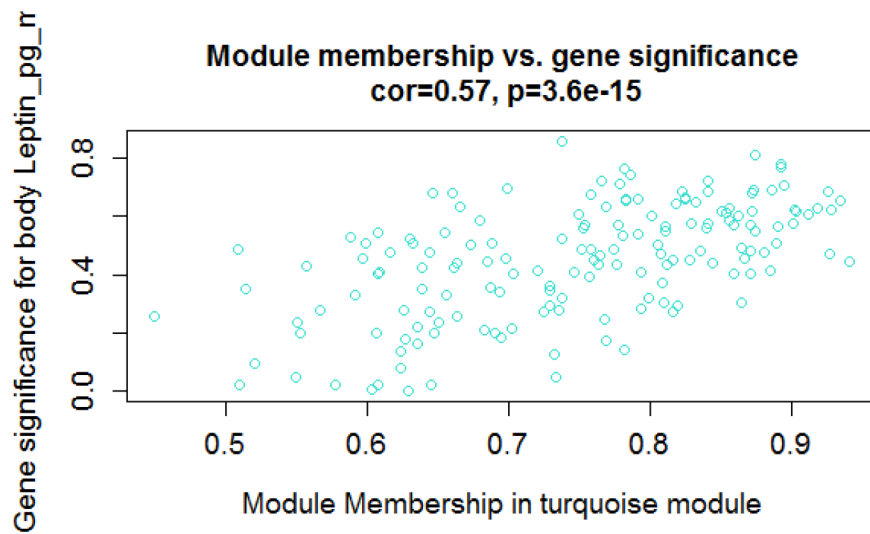
**Supplementary Figure 4. Hierarchical clustering and heatmap of module eigengenes (labeled by their colors) and the triglyceride**



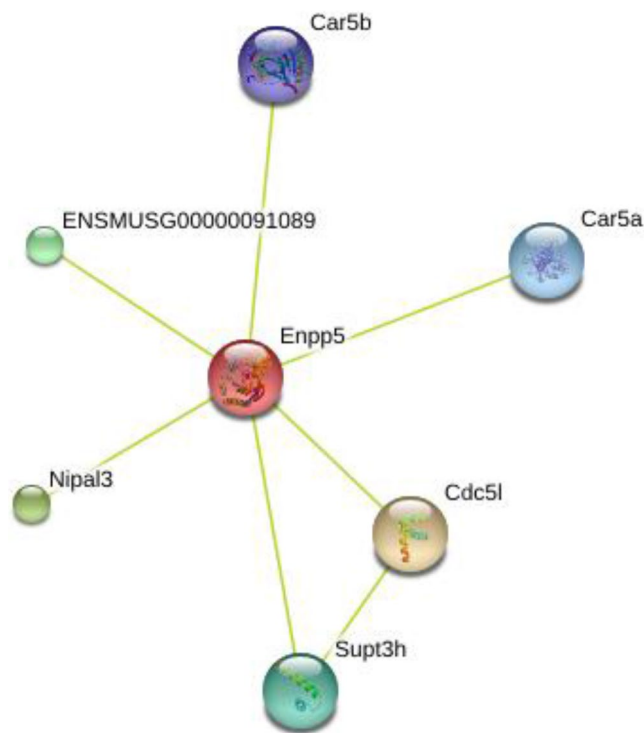
**Supplementary Figure 5. Preservation statistics in age-related vascular aging data (GSE50833).** The size of the bubble represents module size in the data subset used to assess module preservation. The horizontal lines indicate the Z-summary.preservation thresholds for strong evidence of conservation (above 10) and for low to moderate evidence of conservation (above 2). (A) Z-summary.preservation related to module size (B) relationship between the two preservation statistics (Z-summary.preservation and medianRank). Lower medianRank indicates higher preservation.



**Supplementary Figure 6. Scatterplot shows a highly significant correlation between gene significant (GS) versus module membership (MM) in the blue module with free fatty acid (FFA).**



**Supplementary Figure 7.** Scatterplot shows a highly significant correlation between gene significant (GS) versus module membership (MM) in the turquoise module with leptin.



**Supplementary Figure 8.** Protein-protein interaction network of Enpp5 gene.



## Supplementary Tables

Please browse Full Text version to see the data of Supplementary Tables 1–21.

**Supplementary Table 1.** Normalized values for agilent TXT files of GSE50833 with quantile method.

**Supplementary Table 2.** Differentially expressed genes with p-value < 0.05 between 6 and 20 months old mice.

**Supplementary Table 3.** 1036 significantly differentially expressed genes between 3 32-week and 3 78-week old wild-type mice ( $P \leq 0.05$ ) from a study by Gräbner et al., (2009)

**Supplementary Table 4.** 125 genes matched to modules defined by dataset GSE10000.

**Supplementary Table 5.** GO enrichment terms of the genes within the significant modules.

**Supplementary Table 6.** Promoter analysis of the 30 hub genes in the turquoise module by iRegulon.

**Supplementary Table 7.** Promoter analysis of the 30 hub genes in the blue module by iRegulon.

**Supplementary Table 8.** Promoter analysis of the 30 hub genes in the red module by iRegulon.

**Supplementary Table 9.** Promoter analysis of the 90 hub genes in the turquoise, blue and red modules.

**Supplementary Table 10.** Module membership (MM) of genes within the modules and gene significance (GS) in the turquoise module and triglyceride.

**Supplementary Table 11.** Module membership (MM) of genes within the modules and gene significance (GS) in the blue module and free fatty acid (FFA).

**Supplementary Table 12.** Module membership (MM) of genes within the modules and gene significance (GS) in the turquoise module and leptin.

**Supplementary Table 13.** Cytoscape-format node list for the turquoise-blue modules.

**Supplementary Table 14.** Cytoscape-format edge list for the turquoise-blue modules.

**Supplementary Table 15.** Betweenness centrality analysis of genes within the turquoise-blue modules with CytoNCA.

**Supplementary Table 16.** Edge list of genes within blue module that is read in VisANT.

**Supplementary Table 17.** Edge list of top 30 genes within the blue module that is read in VisANT.

**Supplementary Table 18.** Edge list of genes within the red module that is read in VisANT.

**Supplementary Table 19.** Edge list of top 30 genes within red module that is read in VisANT.

**Supplementary Table 20.** Edge list of genes within the turquoise module that is read in VisANT.

**Supplementary Table 21.** Edge list of top 30 genes within the turquoise module that is read in VisANT.